Electrochemical Properties of Langmuir−Blodgett Mixed Films Consisting of a Water-Soluble Porphyrin and a Phospholipid

I. Prieto,[†] M. T. Martín,[†] D. Möbius,[‡] and L. Camacho*[,†]

Departamento de Química Física y Termodinámica Aplicada, Universidad de Córdoba, 14004 Córdoba, Spain, and Max-Planc-Institut für biophysikalische Chemie, Am Fassberg 11, D-370 77, Germany

Received: October 9, 1997; In Final Form: December 26, 1997

Films of a water-soluble tetracationic porphyrin (TMPyP) and an insoluble phospholipid (DMPA), in a molar ratio TMPyP:DMPA = 1:4, were transferred onto optically transparent indium tin oxide (ITO) electrodes, and cyclic voltammetry and visible spectroscopy were used to detected and quantify the presence of porphyrin on the ITO supports. We found the surface density of porphyrin deposited ranges from that corresponding to a monolayer of porphyrin monomers lying parallel to the electrode surface to the total amount of porphyrin (partially as dimer) present in the compressed monolayer at the air−water interface. Also, the electrochemical properties of the films were analyzed in terms of experimental variables including the nature and concentration of the electrolyte and the scan rate, used to obtain the voltammetric recordings. When the reduction of TMPyP is a two-electron process and the salt concentration moderate, porphyrin remains anchored to the phospholipid film, which makes the system highly stable and reversible in successive oxidation−reduction cycles.

Introduction

The electrochemical properties of monolayers and Langmuir−Blodgett (LB) films have aroused much interest from researchers over the past decade.[1−5] The LB technique allows one to obtain surface films of a high internal order, select the number of monolayers that are to form the film, and alternate monolayers of the same or different composition, among others. By careful control of these variables, one can derive useful information on charge-transfer mechanisms in highly organized systems.[6,7]

The formation of LB films requires the use of amphiphilic molecules; however, some methods allow a wide variety of nonamphiphilic molecules−water-soluble substances included−to be used for this purpose.[8−11] Such methods construct complex monolayers consisting of supramolecular structures where the monolayer components are organized by external control taking into account intermolecular interactions that are specific for each system.

In previous work,[12] we obtained mixed monolayers by using the cospreading method[13−16] with a water-soluble tetracationic porphyrin (TMPyP) and an insoluble phospholipid matrix containing an anionic polar group (DMPA). The structures of these components are shown in Scheme 1.

The optimum molar ratio for the formation of TMPyP:DMPA monolayers was found to be 1:4, which corresponds to the stoichiometry of the molecular charges of the components. The results obtained for this mixture reveal that all porphyrin molecules are retained on the phospholipid matrix via charge interactions at the air−water interface; the molecules arrange themselves in such a way that the central ring of porphyrin lies parallel to the interface.[12] At high surface pressures, the area occupied by each porphyrin molecule in this configuration exceeds that of four phospholipid molecules; this results in a complex monolayer arrangement where the porphyrin molecules stack as depicted in Scheme 2A.[12]

SCHEME 1: Structures of the Molecules Studied

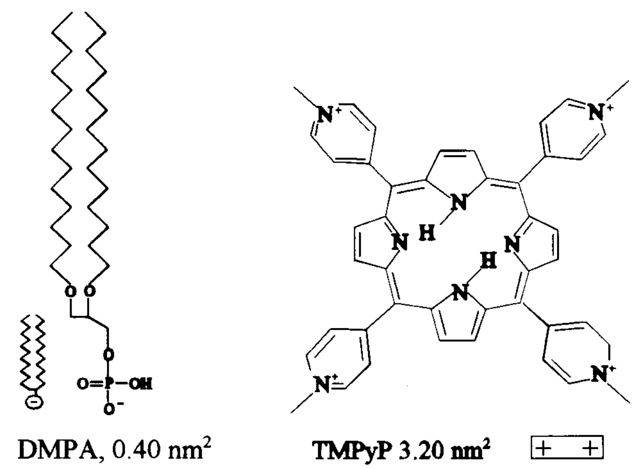

SCHEME 2: (A) Stacked Structure of the Porphyrin Dimer and (B) Structure of the TMPyP:DMPA = 1:4 Monolayer at the Air−Water Interface and on Glass

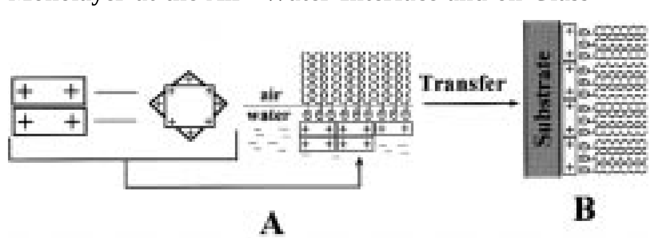

The above-mentioned TMPyP:DMPA = 1:4 films were transferred from the air−water interface at a surface pressure of 35 mN/m, where about 90% of all porphyrin molecules are present as dimers on hydrophilic glass. This support only receives a monolayer of porphyrin monomer that coincides with the monolayer directly bound to the phospholipid (see Scheme 2B).[12]

* Corresponding author. E-mail: qf1cadel@lucano.uco.es.
[†] Universidad de Córdoba.
[‡] Max-Planc-Institut für biophysikalische Chemie.

S1089-5647(97)03284-7 CCC: $15.00
Published on Web 03/12/1998

In this work, films of TMPyP:DMPA, in a molar ratio of 1:4, were transferred onto optically transparent indium tin oxide (ITO) electrodes, and cyclic voltammetry and visible spectroscopy were used to detected and quantify the presence of porphyrin on the ITO supports.

Our aim is investigate both the electrochemical properties and the stability of the formed films, in terms of experimental variables including the nature and concentration of the electrolyte and the scan rate, used to obtain the voltammetric recordings.

The porphyrin molecules in films deposited on ITO are encapsulated between the electrode surface and the phospholipid monolayer (Scheme 2B). The redox conversion of the porphyrin molecules requires the rapid insertion or removal of ions across the monolayer. Occasionally, the migration of the counterion across the film can be the rate-determining step in the electron-transfer process.[3,17] In our case, however, the reaction electrode is never controlled by the rate of ion penetration into the film because the ionic migration through the phospholipid monolayer is fast.

The fabrication of electrodes modified with TMPyP/DMPA films has the purpose of showing new methods of immobilization redox centers on electrodes. By the described method, molecules of different types, including water soluble, are attached to a phospholipid matrix by electrostatic interaction. Using particular experimental conditions, the transferred films show a high stability after consecutive oxido-reduction cycles.

Experimental Section

Surface films were transferred from the air–water interface onto a solid support on a computer-controlled Lauda Filmwaage FW2 Langmuir balance supplied with a Lauda Film Lift FL 1 mechanical arm. Films were all transferred at a pressure of 35 mN/m and a support emersion rate of 5 mm/min. The transfer ratio was close to unity in every case. Other experimental conditions used to organize the surface films at the air–water interface are described elsewhere.[12]

Under no polarized light, UV–visible absorption spectra were recorded on a Perkin-Elmer Lambda 3B spectrophotometer. ITO supports, coated with transferred monolayers, were placed in the light path, and a clean support was used as reference. The supports were transparent to visible light and consisted of a glass plate that was vacuum-coated with a mixture of In and Sn oxides $[(In_2O_3)_{\sim 0.88}(SnO_2)_{\sim 0.12}]$ with semiconductor properties.

Cyclic voltammetric recordings were obtained by using a PAR M273 potentiostat. All voltammograms were recorded in a cyclic manner from a preset potential E_0 to the final potential E_f. Platinum and Ag/AgCl were used as auxiliary and reference electrodes, respectively. The working electrodes were ITO electrodes (Balzers Ltd.) coated with TMPyP:DMPA films. IR ohmic drop was uncompensated. All electrochemical experiments were carried out in a nitrogen atmosphere at 21 °C.

5,10,15,20-Tetrakis(1-methyl-4-pyridyl)-21*H*,23*H*-porphyrin (TMPyP, Aldrich), L-α-dimyristoylphosphatidic acid (DMPA, Sigma), and methyl palmitate (PME, Merck) were used without further purification. All other reagents were Merck a.g. and used as supplied. Ultrapure water from a Millipore Milli-Q-Plus system was used throughout.

ITO substrates were previously sonicated in acetone for 15 min, followed by rinsing with water, ultrasonic agitation in concentrated NaOH in 1:1 V/V water/ethanol, rinsing with further water, immersion in Cl_3CH for 10 min, and drying.

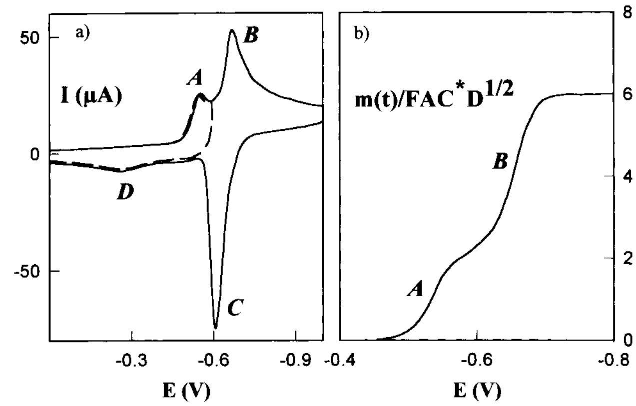

Figure 1. (*a*) Cyclic voltammograms for an aqueous solution of 5×10^{-5} M TMPyP and 0.1 M LiCl on an ITO electrode. $A_{ITO} = 1$ cm^2, $E_0 = 0$ mV, $v = 100$ mV/s, and $T = 21$ °C. (b) Plot of $m(t)/FAC^*D^{1/2}$ against E.

Results and Discussion

Electrochemical Behavior of TMPyP in Solution. The reduction of TMPyP in aqueous media has been previously studied using Hg electrode.[19] The results obtained on this electrode are described below. Using voltammetry, the porphyrin shows two reduction waves at pH = 2 in 10^{-2} M HCl (see Figure 4A from ref 19). The first reduction wave corresponds to a reversible bielectronic process with a peak potential close to −50 mV vs Ag/AgCl. The second reduction wave is tetraelectronic and irreversible with a peak potential close to −600 mV. At pH = 6 in piperazine N,N′-bis(2-ethanesulfonic acid) 0.1 M medium, the bielectronic wave appears at a peak potentials close to −450 mV, keeping constant the peak potential for the second wave. It is emphasized that both reduction waves are irreversible at this pH (see Figure 4C from ref 19). The first wave has been related[19,20] to the two-electron reduction of the central ring of porphyrin, whereas the second has been ascribed to the four-electron reduction of the 1-methyl-4-pyridyl groups.[19,20]

TMPyP electrochemical behavior had never been studied on ITO electrode. Prior to the electrochemical study of TMPyP supported on ITO, we analyzed its behavior in aqueous solutions in order to be able to characterize the overall electrode process. The solid line in Figure 1a is the cyclic voltammogram obtained for 5×10^{-5} M TMPyP in an aqueous solution containing 0.1 M LiCl, where the final potential was −1 V.

The voltammogram was recorded at a scan rate $v = 100$ mV/s, using an ITO electrode with a surface area $A = 1$ cm^2 as the working electrode. The area was previously calibrated with ferrocyanide solutions of known diffusion coefficient.[18] As can be seen, the voltammogram exhibits two reduction peaks at potentials close to −550 (peak A) and −650 mV (peak B), respectively. Similar peaks were previously obtained with an Hg electrode at pH 6 (see Figure 4C in ref 19); however, the peaks provided by this type of electrode appear at slightly more positive potentials.

As can also be seen, the voltammogram of Figure 1a exhibits two oxidation peaks; the more negative peak (peak C) appears close to −600 mV and possesses the narrow sharp shape typical of a precipitate stripped from an electrode. The more positive oxidation peak (peak D) is smaller and broader than the previous one and appears at potentials close to −300 mV. The dashed line in Figure 1a shows a cyclic scan finished immediately after peak A (−595 mV); as can be seen, peak D is again observed, but peak C is not. It should be noted that peaks C and D are

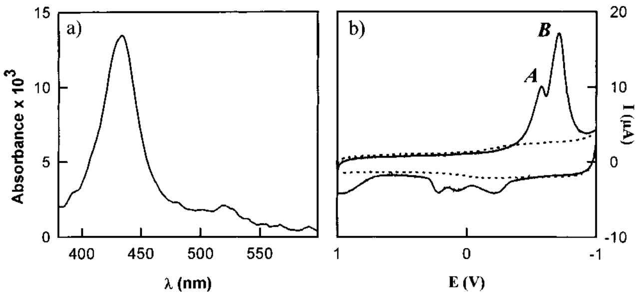

Figure 2. (a) UV−visible absorption spectrum for a TMPyP:DMPA = 1:4 monolayer. (*b*) Cyclic voltammograms for a TMPyP:DMPA = 1:4 monolayer deposited on an ITO electrode immersed in a 10^{-4} M $KClO_4$ solution (solid line) and for an uncoated ITO electrode (dashed line). $A_{ITO} = 0.5$ cm^2, $E_0 = 1000$ mV, $v = 100$ mV/s, and $T = 21$ °C.

not present in scans of an Hg electrode at pH 6—at least under the experimental conditions used in ref 19.

With an Hg electrode at pH 6, the overall reduction of TMPyP involves the uptake of six electrons per molecule;[19,20] peak A corresponds to a two-electron process and peak B to a four-electron one. We checked this experimentally by determining the semi-integral of the current corresponding to a whole reduction scan, $m(t)$,[21−26] which is shown in Figure 1b. The semi-integral calculation, eq 1, allows one to determine the number of electrons exchanged in each reduction process provided diffusion control prevails and the diffusion coefficient, D_A, is known. We calculated the difussion coefficient to be $D_A \approx 3.3 \times 10^{-6}$ cm^2/s from voltammetric recordings in an acid medium (pH 2), where TMPyP gives rise to a reversible two-electron wave at potentials close to −50 mV.[19]

$$m(t) = \frac{1}{\sqrt{t}}\int_0^t \frac{I\,du}{\sqrt{t-u}} = nFA\sqrt{D_A}C^*\left[1 - \frac{C(0,t)}{C^*}\right] \quad (1)$$

In this equation, I is the reduction current, t time, A the area of the electrode, F the Faraday constant, n the number of electrons exchanged per molecule, C^* the concentration of TMPyP in solution, and $C(0,t)$ that of porphyrin on the electrode surface. In Figure 1b is plotted $m(t)/FAC^*D_A^{1/2} = n[1 - C(0,t)/C^*]$ versus potential (E). $C(0,t)$ decreases with increasing potential and is zero at potentials corresponding to the diffusion zone, i.e., for appropiate negative potential values.

Beyond peaks A and B the process gives rise to two waves (see Figure 1b), the heights of which after semi-integration reveal the exchange of two and four electrons per molecule, respectively, similarly as with the Hg electrode.[19]

Stability and Analysis of TMPyP/DMPA Films Deposited on ITO. At the transfer pressure used (35 mN/m), the area per porphyrin molecule at the air−water interface at the time of transfer was 1.92 nm^2, which is equivalent to a surface concentration $\Gamma = 8.65 \times 10^{-11}$ mol/cm^2. This concentration is higher than the theoretically expected value for a compact monolayer consisting of porphyrin monomers lying coplanar with the interface, $\Gamma_m = 5.19 \times 10^{-11}$ mol/cm^2, which was estimated on the assumption of a molecular plane area of 3.2 nm^2.[12,27]

Figure 2a shows an absorption spectra for an ITO coated with a monolayer of TMPyP:DMPA = 1:4. The spectra were typical of the used porphyrin[12] and exhibited a Soret band maximum close to 427−430 nm, which confirms the presence of porphyrin the monolayer.[12]

In all the experiments performed, the full width at half-maximun is constant; however, the maximum absorbance values were highly disperse (from 0.012 to 0.019).

Prior to electrochemical experiments, we analyzed the stability in solution of monolayers transferred onto ITO. For this purpose, we recorded absorption spectra for freshly deposited surface films. Then, the films were immersed in aqueous solutions containing variable salt concentrations. After a preset time, the ITO electrode was removed from the solution and dried, and a new absorption spectrum for the monolayer was recorded. The experiments revealed that, in the presence of perchlorate ions, the absorption spectra obtained prior to and after immersing the ITO electrode in the solution were essentially similar regardless of the cation present as counterion in the medium and the immersion time used. This suggests that no porphyrin molecules are transferred from the monolayer into the solution. By contrast, the presence of chloride ions decreased the spectral maximum (by 30−40% after 5 min of immersion in 0.1 M LiCl). The high stability of the monolayers in the perchlorate medium appears to be related to the fact that TMPyP is highly insoluble in aqueous solutions of this salt but highly soluble in chloride solutions. For this reason, the electrochemical study of TMPyP:DMPA monolayers was conducted exclusively in perchlorate media.

The ITO electrode, coated with a TMPyP:DMPA = 1:4 monolayer, was immersed in perchlorate solution and used, untreated, as the working electrode in a conventional electrochemical cell. The solid line in Figure 2b shows a cyclic voltammogram for this system obtained at $v = 100$ mV/s in 10^{-4} M $KClO_4$. The figure also shows a voltammogram recorded under the same conditions by using a bare ITO electrode (dotted line). As can be seen, reduction peaks A and B are clearly resolved in the voltammogram; however, there are marked differences from the behavior of porphyrin in solution (Figure 1a). Thus, at potentials more negative than that where peak B appears, the current drops to the background as a result of the whole monolayer being reduced. Also, the oxidation scan produces up to four different peaks, the position and height of which depend strongly on the electrolyte concentration used, as well as on the scan rate, as shown later.

Integrating the reduction current allows one to determine the total amount of charge exchanged, Q, which in turn can be related to the surface concentration of porphyrin (Γ):

$$Q = (1/A)\int I\,dt = nF\Gamma \quad (2)$$

Q has been calculated by integration of the measured peaks once the background current has been removed. The procedure extrapolated linearly the charge current from potentials immediately more positive than those corresponding to the appearance of the peak A to potentials immediately more negative than those found for the peak B. The values of Q obtained by this procedure present a negligible difference with respect to those calculated when the current measured for the monolayer is directly subtracted from that for clean ITO electrode.

Like the previous absorbance values, the charge values obtained for the first reduction cycle were also highly disperse (from 27 to 52 μC/cm^2). Figure 3 shows a plot of absorbance versus charge values (white circles) obtained in about 50 different experiments that involved preparing each monolayer and recording its absorption spectrum and cyclic voltammogram.

The solid line in the Figure 3 shows the linear regression of the experimental data set. It should noted that the line has a nonzero intercept, which suggests that the charge is not directly proportional to the absorbance.

Figure 3 also shows two vertical dotted lines, the first of which corresponds to the charge one would expect if a single

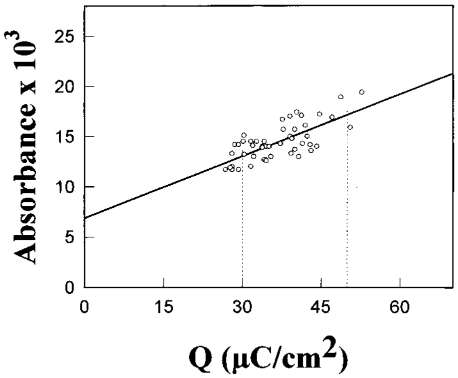

Figure 3. Plot of absorbance values against the electrochemical charges obtained for different TMPyP:DMPA = 1:4 monolayers (white circles) deposited on ITO. The solid line represents the linear regression of the experimental. The vertical dotted lines correspond to the charge values 30 and 50 μC/cm^2.

whole monolayer of porphyrin monomer were transferred onto the ITO electrode, i.e., if $\Gamma_m = 5.19 \times 10^{-11}$ mol/cm^2; under these conditions, eq 2 with $n = 6$ yields $Q_m = 30$ μC/cm^2. The second vertical line corresponds to the charge one would expect if every porphyrin molecule at the air−water interface were transferred onto the ITO electrode at the transfer pressure, i.e., if $\Gamma = 8.65 \times 10^{-11}$ mol/cm^2; under these conditions, eq 2 yields $Q = 50$ μC/cm^2.

As can be seen in Figure 3, experimental charges ranged from the values expected if only the porphyrin molecules of a monomer monolayer were transferred onto the electrode to those expected if all the molecules of porphyrin at the air−water interface were transferred. This phenomenon could be ascribed to decreasing with time of the surface activity toward porphyrin adsorption. Thus, electrodes purchased shortly before used, having a surface that still preserved the properties of the vacuum-deposited semiconducting material, received all the porphyrin molecules present at the air−water interface and produced experimental charge values close to 50 μC/cm^2 (see Figure 3). After each electrochemical experiment, the ITO electrodes were cleaned by following the procedure described in the Experimental Section and used to transfer new porphyrin monolayers. As each electrode was reused, the number of porphyrin molecules that were deposited on its surface was found to gradually decrease. Thus, a single monolayer was transferred after only three or four experiments. Beyond that point, the ITO surface behaved similarly to a glass surface with respect to the monolayer transfers.[12] Although surface properties of ITO change with increasing number of experiments, the electrochemical properties of the ITO remain constant.

It is a fact that the absorbance and Q are not directly proportional in magnitude (see Figure 3) and this must be related to the partial formation of dimer by the TMPyP, whose molar absortivity is lower than that of monomer as observed at the air−water interface.[12] Thus, the molar fraction of dimer has to increase with increase of the surface concentration of porphyrin and consequently a decrease of the molar absortivity of the film is obtained.

Electrochemical Behavior of the TMPyP/DMPA System on ITO. As noted earlier, TMPyP:DMPA = 1:4 monolayers deposited on ITO are highly stable while immersed in a perchlorate solution. The following sections discuss the influence of the type of cation used, the concentration of electrolyte and the scan rate at which the voltammogram is performed.

Influence of the Type of Electrolyte. Table 1 shows the potentials of peaks A and B (see Figure 2) produced by a TMPyP:DMPA = 1:4 monolayer deposited on ITO in a medium containing various perchlorate salts at a 10^{-2} M concentration, at $v = 100$ mV/s. The values in the table were subject to an experimental oscillation of ±10 mV among experiments. Broadly speaking, the type of cation used hardly affects the shape or size of the voltammetric peaks obtained except for small variations in the potentials of peaks A and B.

TABLE 1: Potentials of Peaks A and B for Different TMPyP:DMPA = 1:4 Monolayers Deposited on ITO[a]

salt	E_p(A) (mV)	E_p(B) (mV)
TEAP	−500	−617
$KClO_4$	−508	−635
$NaClO_4$	−525	−645
$LiClO_4$	−487	−620

[a] $C_{salt} = 10^{-2}$ M, $v = 100$ mV/s.

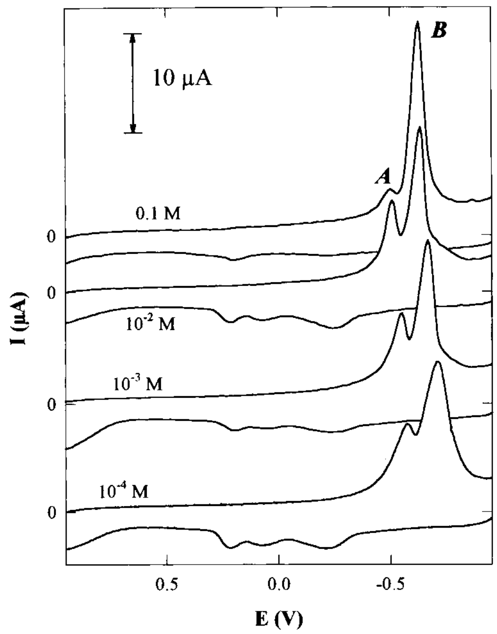

Figure 4. Cyclic voltammograms for different TMPyP:DMPA = 1:4 monolayers deposited on an ITO electrode immersed in $KClO_4$ at a variable concentration of the supporting electrolyte (from top to bottom: 0.1, 10^{-2}, 10^{-3}, and 10^{-4} M). $A_{ITO} = 0.5$ cm^2, $E_0 = 1000$ mV, $v = 100$ mV/s, and $T = 21$ °C.

Influence of the Electrolyte Concentration. Figure 4 shows four voltammograms obtained for different TMPyP/DMPA=1:4 monolayers at variable $KClO_4$ concentrations in the medium and $v = 100$ mV/s.

As can be seen in the reduction scans, peak A is smaller in 0.1 M $KClO_4$ than at all other concentrations tested. The inhibition of peak A is more marked at decreased scan rates; in fact, peak A virtually disappears in 0.1 M $KClO_4$ at $v = 10$ mV/s, where peak B is stronger than under other conditions (data not shown). This inhibition of peak A is also demonstrated when the areas of peaks A and B are compared, once the background current is subtracted. In fact, theoretically the area under peak A has to be half of that under peak B since two and four electrons, respectively, are exchanged (see Figure 1). However, the experimental area from peak A is always smaller than that expected. The inhibition of peak A only seems to disappear when a very low concentration of supporting electrolyte or high scan rate is used, and then, the theoretical ratio between the areas of peaks A and B tends to achieve.

In the reduction scan, it is also possible to observe that at extremely low concentrations of perchlorate, 10^{-4} M, peaks A and B widen and shift slightly to more negative potentials. This

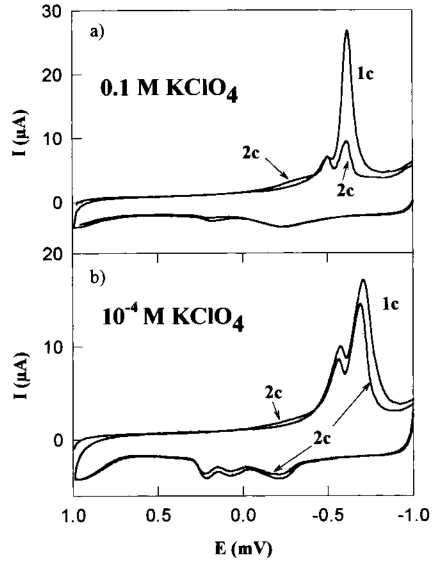

Figure 5. Cyclic voltammograms for different TMPyP:DMPA = 1:4 monolayers deposited on an ITO electrode immersed in a $KClO_4$ solution at a variable concentration of the supporting electrolyte: (a) 0.1 M; (b) 10^{-4} M; first cycle (1c), second cycle (2c). $A_{ITO} = 0.5$ cm^2, $E_0 = 1000$ mV, $\upsilon = 100$ mV/s, and $T = 21$ °C.

behavior has to be attributed both to the uncompensated IR drop through the cell and to the effects of the double layer.[28] In this work, the influence of those phenomena on voltammograms has not been corrected, since the kinetic parameters have not been determined. In any case, such influence is not very important and only has an affect when a low concentration of perchlorate ($\leq 10^{-4}$ M) is used.

The oxidation scans of Figure 4 exhibit up to four peaks at potentials close to −250, +60, +200, and +960 mV. The most positive peak cannot be precisely resolved owing to its proximity to the electrode's anodic limit (ca. +1 V). All these peaks decrease in size as the $KClO_4$ concentration is raised; thus, only the peak at about +200 mV is clearly observed in the scans done in 0.1 M $KClO_4$.

Figure 5 shows the first two voltammetric cycles performed in a consecutive manner in 0.1 and 10^{-4} M $KClO_4$.

The reduction current obtained in 0.1 M $KClO_4$ (Figure 5a) at $\upsilon = 100$ mV/s for the second cycle (2c) is considerably smaller than that for the first (1c). This must be related to the virtually complete disappearance of the oxidation peaks during the first voltammetric cycle. By contrast, the first (1c) and second reduction cycle (2c) in 10^{-4} M $KClO_4$ are very similar; in fact, the signal obtained in the second cycle is only slightly smaller (about 10%) than that recorded in the first.

The solid line in Figure 6 shows the first two voltammetric cycles performed in 10^{-4} M TEAP at $\upsilon = 100$ mV/s and a final potential immediately following that of appearance of peak A.

Actually, the solid line represents two consecutive cycles. Obviously the signals of both cycles are identical. The oxidation scan of this voltammogram exhibits a peak near −300 mV, which is close to the potential of appearance of peak D for dissolved TMPyP (see Figure 1a). The dotted line in Figure 6 shows a voltammogram taken of the same electrode after the two scans at $E = -550$ mV. As can be seen, the final potential is beyond that of appearance of peak B in this case. Also, the signal corresponding to peak A coincides with the previous recordings, and the oxidation peak at ca. −300 mV is not observed. The electrochemical behavior reflected in Figure 6 was observed with the four perchlorate salts used as supporting electrolyte.

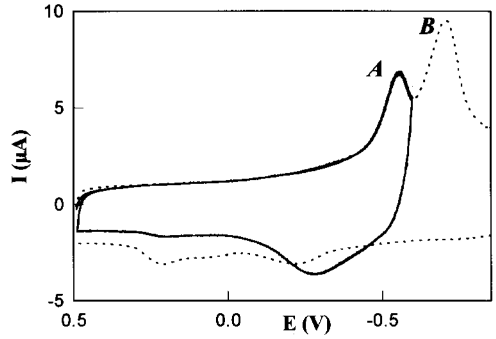

Figure 6. Cyclic voltammograms for a TMPyP:DMPA = 1:4 monolayer deposited on an ITO electrode immersed in a 10^{-4} M TEAP solution at $E_f = -590$ mV (solid line, two cycles) and $E_f = -1000$ mV (dashed line). $A_{ITO} = 0.5$ cm^2, $E_0 = 500$ mV, $\upsilon = 100$ mV/s, and $T = 21$ °C.

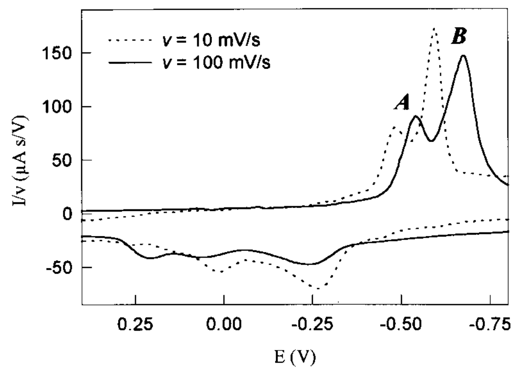

Figure 7. Plot of I/υ vs υ obtained from the cyclic voltammograms for different TMPyP:DMPA = 1:4 monolayers deposited on an ITO electrode immersed in a 10^{-3} M TEAP solution, at two different scan rates: 100 mV/s (solid line) and 10 mV/s (dashed line). $A_{ITO} = 0.5$ cm^2, $E_0 = 500$ mV, and $T = 21$ °C.

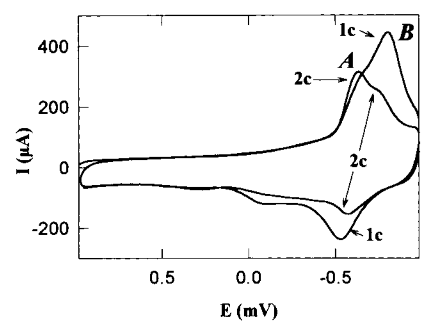

Figure 8. Cyclic voltammogram for a TMPyP:DMPA = 1:4 monolayer deposited on an ITO electrode immersed in a 0.1 M TEAP solution: first cycle (1c), second cycle (2c). $A_{ITO} = 0.5$ cm^2, $E_0 = 1000$ mV, $\upsilon = 5$ V/s, and $T = 21$ °C.

Influence of the Scan Rate. Figure 7 shows two cyclic voltammograms obtained at a variable scan rate in 10^{-3} M TEAP in the form of an I/υ versus E plot for easier comparison of the voltammograms.

In the reduction scan, peaks A and B shift to more negative potentials (by about −60 and −80 mV per decade, respectively) as the scan rate is increased. In the oxidation scan performed at $\upsilon = 10$ mV/s, the peak at about +200 mV disappears while the other signals increase and are shifted to more negative potentials relative to the voltammogram recorded at $\upsilon = 100$ mV/s.

Some of the above-described phenomena are strongly dependent on the scan rate used. Figure 8 shows the first two voltammetric cycles obtained in 0.1 M $KClO_4$ at $\upsilon = 5$ V/s.

SCHEME 3: Changes in the Monolayer Composition by Effect of Its Two-Electron (Peak A) and Six-Electron Reduction (Peaks A + B)

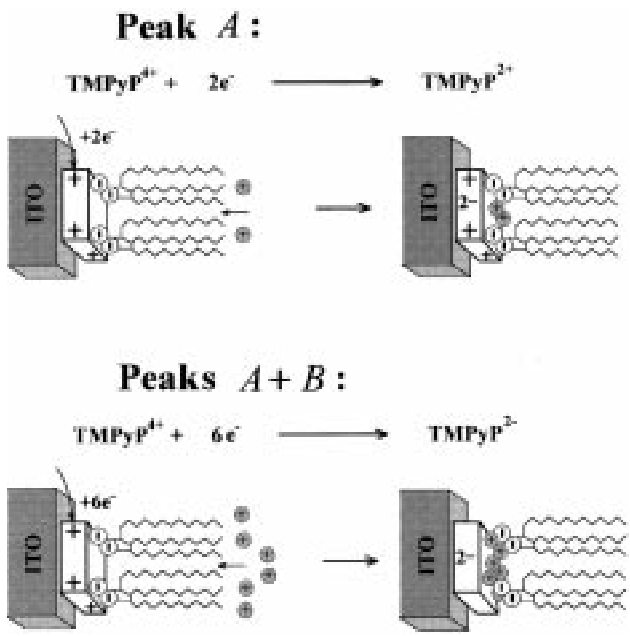

As can be seen, the first reduction scan leads to sharp peaks A and B. The corresponding oxidation scan exhibits one peak at −500 mV not observed in the voltammograms obtained at v = 100 mV/s (see Figures 4−7). The potential for this oxidation peak is similar to that for peak C of TMPyP in an aqueous medium (see Figure 1a) except for a slight shift to more positive potentials that can be ascribed to the different scan rate used.

In the second cycle of the voltammogram of Figure 8, peak A appears at slightly more positive potentials and is similar in size to that observed in the first cycle. By contrast, peak B is considerably smaller—it decreases in the second oxidation by roughly the same degree as do the peaks observed in the first cycle.

Scan rates up to 20 V/s have been used, and no differences have been found with respect to that described in Figure 8.

Interpretation of the Electrochemical Behavior Observed. We conclude from the voltammetric behavior at high scan rate (up to 20 V/s), that the electrode reaction is never controlled by the rate of the anion penetration to the film. Under these experimental conditions (see Figure 8), the electrode process of porphyrin exhibits a redox behavior similar to that observed in an aqueous medium (see Figure 1).

The six-electron reduction of porphyrin (peaks A + B) begins with the uptake of two electrons by the central ring of the substrate (peak A), followed by the disappearance of the four positive charges of the 1-methyl-4-pyridyl groups (peak B) resulting in a repulsing interaction between the porphyrin and the DMPA monolayer (see Scheme 3). In any case, hexareduced porphyrin remains on the electrode because, as can be inferred from its electrochemical behavior in water (see peak C in Figure 1), it is insoluble in this medium.

In its two-electron reduction (peak A), porphyrin preserves the four positive charges of its 1-methyl-4-pyridyl groups since the reduction affects the central ring only[19,20] (see Scheme 3). Such positive groups are used to anchor the porphyrin to the phospholipid matrix. In this case, the electrode process behaves similarly as in solution—compare the voltammogram represented by the dashed line of Figure 1 with the solid line of Figure 6; also, successive voltammetric cycles on the monolayers produce identical signals. This behavior suggests that porphyrin molecules are not displaced from their charged complex with DMPA; the monolayers are highly stable under these conditions, at least at low concentrations of the supporting electrolyte.

The influence of the supporting electrolyte on the electrode process is complex as can be inferred from the observed inhibition of peak A (see Figure 4) at high perchlorate concentration. A possible explanation for such inhibition could be related to the break of the charge complex formed between DMPA and the porphyrin due to the massive penetration of ions from the solution to the monolayer.

Conclusions

We transferred monolayers of TMPyP:DMPA = 1:4 from the air−water interface onto ITO at a surface pressure of 35 mN/m. The surface density ranges from that corresponding to a monolayer of porphyrin monomers lying parallel to the electrode surface to the total amount of porphyrin present in the compressed monolayer at the air−water interface.

Phospholipid (DMPA) films on ITO are highly permeable to ions; even at high scan rate (20 V/s), the electrode reaction is never controlled by the rate of the anion penetration into the film.

When the reduction of TMPyP is a two-electron process (peak A) and the salt concentration low, porphyrin remains anchored to the phospholipid film, which makes the system highly stable and reversible in successive oxidation−reduction cycles. On the other hand, when TMPyP is reduced in a six-electron process (peaks A + B), porphyrin is released from the phospholipid matrix. Under these conditions, the oxidation of porphyrin and the return to its initial position in the monolayer are incomplete, depending on the particular experimental conditions, and consequently the electrochemical signal decreases gradually to a variable extent in successive oxidation−reduction cycles. Thus, peak A is inhibited when both a high concentration of supporting electrolyte and low scan rate are used. This phenomenon will be due to the breaking of the charge complex formed between DMPA and the porphyrin.

Acknowledgment. The authors express their gratitude to the Spanish DGICyT for financial support (Projects PB94-0446).

References and Notes

(1) Murray, R. W. In *Molecular Design of Electrode Surfaces*; Murray, R. M., Ed.; John Wiley & Sons, Inc.: New York, 1992; p 1.
(2) Facci, J. S. In ref 1, p 119.
(3) Majda, M. in ref 1, p 159.
(4) Mirkin, C. A.; Ratner, M. A. *Annu. Rev. Phys. Chem.* **1992**, *43*, 719.
(5) Goldenberg, L. M. *J. Electroanal. Chem.* **1994**, *379*, 3.
(6) Zhang, X.; Bard, A. J. *J. Am. Chem. Soc.* **1989**, *111*, 8098.
(7) Ueyama, S.; Isoda, S.; Maeda, M. *J. Electroanal. Chem.* **1990**, *293*, 111.
(8) Grüniger, H.; Möbius, D.; Meyer, H. *J. Chem. Phys.* **1983**, *79*, 3701.
(9) Kuhn, H.; Möbius, D. In *Investigations of Surfaces and Interfaces*, 2nd ed.; Rossiter, B. W., Baetzold, R. C., Eds.; John Wiley & Sons, Inc.: New York, 1993; Vol. IXB, p 375.
(10) Akins, D. L.; Zhu, H.-R.; Guo, C. *J. Phys. Chem.* **1994**, *98*, 3612.
(11) Vergeldt, F. J.; Kochorst, R. B. M.; Hoek, A. V.; Schaafsma, T. J. *J. Phys. Chem.* **1995**, *99*, 4397.
(12) Martín, M. T.; Prieto, I.; Camacho, L.; Möbius, D. *Langmuir* **1996**, *12*, 6554.
(13) Hada, H.; Hanawa, R.; Haraguchi, A.; Yonezawa, Y. *J. Phys. Chem.* **1985**, *89*, 560.
(14) Yonezawa, Y.; Möbius, D.; Kuhn, H. *Ber. Bunsen-Ges. Phys. Chem.* **1986**, *90*, 1183.
(15) Cordroch, W.; Möbius, D. *Thin Solid Films* **1992**, *210/211*, 135.
(16) Schoeler, U.; Tews, K. H.; Kuhn, H. *J. Chem. Phys.* **1974**, *61*, 5009.
(17) Petty, M.; Lovett, D. R.; Miller, J.; Silver, J. *J. Mater. Chem.* **1991**, *1*, 971.
(18) Chailapakul, O.; Crooks, R. *Langmuir* **1993**, *9*, 884.

(19) Neri, B. P.; Wilson, G. S. *Anal. Chem.* **1972**, *44*, 1002.
(20) Kadish, K. M.; Araullo, C.; Maiya, G. B., Sazou, D.; Barbe, J.-M.; Guilard, R. *Inorg. Chem.* **1989**, *28*, 2528.
(21) Oldham, K. B. *Anal. Chem.* **1969**, *41*, 1904.
(22) Oldham, K. B. *Anal. Chem.* **1972**, *44*, 196.
(23) Oldham, K. B. *Anal. Chem.* **1972**, *44*, 1121.
(24) Oldham, K. B. *Anal. Chem.* **1973**, *45*, 39.
(25) Goto, M. G.; Oldham, K. B. *Anal. Chem.* **1973**, *45*, 2043.
(26) Goto, M. G.; Oldham, K. B. *Anal. Chem.* **1974**, *46*, 1522.
(27) Möbius, D.; Grüniger, H. R. *Bioelectrochem. Bioenerg.* **1984**, *12*, 375.
(28) Becka, A. M.; Miller, C. J. *J. Phys. Chem.* **1993**, *97*, 6233.